The adsorption and desorption of CdI_2 on InSb(001): observation of an epitaxial orientational relationship

The adsorption and desorption of CdI₂ on InSb(001): observation of an epitaxial orientational relationship

Andrew P Mowbray and Robert G Jones

Department of Chemistry, University of Nottingham, University Park, Nottingham NG7 2RD, UK

Abstract. A LEED, AES and ARUPS study has been made of CdI_2 adsorbed on the clean In-rich InSb(001) c(8 × 2) reconstructed surface at room temperature. A chemisorbed p(2 × 1) structure formed which consisted of a double layer of iodine atoms with cadmium atoms between them. It is suggested that this surface consists of linear I–Cd–I molecules aligned perpendicularly to the surface. Continued adsorption caused growth of an orientational relationship epitaxial layer of CdI_2. The epitaxial layer had the basal plane of the layered CdI_2 material parallel to the InSb(001) surface, with the hexagonal mesh of the CdI_2 at an angle of $\simeq 7°$ to the square net of the substrate. On heating to $\simeq 400$ K the epitaxial layer desorbed leaving a p(2 × 1) structure identical to that formed during adsorption. The p(2 × 1) was stable to 433 K beyond which further loss of Cd and I caused a change to a (1 × 1) structure. This structure is thought to consist of a (1 × 1) monolayer of iodine with Cd below the iodine layer, possibly incorporated into the substrate. Heating to 500 K caused complete loss of iodine and cadmium from the surface and the formation of a clean, Sb-rich surface.

1. Introduction

At one extreme adsorbed species may be regarded as separate particles, either atoms or molecules, with the dominant interaction being that between the particle and the surface. Any lateral interactions between adsorbed particles are then regarded as perturbations of the dominant interaction with the surface. At the other extreme the adsorbed species may have isotropic interactions between themselves which exceed their interactions with the surface and so lead to three-dimensional solid formation and non-wetting behaviour. Between these two extremes we can envisage the growth of an anisotropic material (a layered compound) on an isotropic solid. Such a layered compound gives a stack of monolayers with strong intra-layer bonding and weak inter-layer bonding. One such layer adsorbed on a surface will exhibit competition between site adsorption, due to interaction with the substrate, and incommensurate adsorption due to the strength of the lateral interactions. One might also expect to see an orientational relationship between the layered material and the substrate to reduce the interfacial energy to a minimum. In this paper we explore this idea using the layered material cadmium iodide (CdI_2) adsorbed on InSb(001). Cadmium iodide is one of the simplest, easily evaporable, layered materials available. The only simpler ones are elemental graphite and white boron nitride, both of which require high evaporation temperatures, and possibly As_2O_3 (claudetite) which has puckered layers consisting of As bonded through oxygen atoms.

Cadmium iodide has already been extensively studied with respect to its layer-like, two-dimensional band structure [1, 2]. It has a structure which consists of a strongly bound double layer of iodine with cadmium in the octahedral holes, each I–Cd–I sandwich layer being bonded to the layers above and below by relatively weak van der Waals forces. The melting point and boiling point of the pure material are 660 K and 1069 K respectively [3].

The InSb(001) surface used in this study was the indium-rich $c(8 \times 2)$ reconstruction, which is thought to consist of $\frac{3}{4}$ ML of In as dimers plus a missing dimer site, sitting on top of an unreconstructed (1×1) Sb layer [4] (1 ML is defined here as a 1:1 correspondence of adspecies to Sb (or In) atoms in a crystallographic plane). A second clean surface structure, variously referred to as a streaky (4×2) or a (4×1) [5], was also used and behaved identically to the $c(8 \times 2)$. The streaky $(4 \times 2)/(4 \times 1)$ structure is simply a disordered version of the $c(8 \times 2)$ [5].

In this paper the growth and destruction of the CdI_2 layer on the InSb(001) was monitored using low-energy electron diffraction (LEED), Auger electron spectroscopy (AES) and angle-resolved ultraviolet photoelectron spectroscopy (ARUPS). The first complete layer of CdI_2 lifts the surface reconstruction and forms a sharp $p(2 \times 1)$ structure. This structure, which has an electronic structure markedly different to that of bulk CdI_2, contains two molecules of CdI_2 per $p(2 \times 1)$ unit mesh, and probably consists of linear I–Cd–I species aligned vertically on the surface. Further adsorption then leads to the formation of a rather well formed epitaxial layer of CdI_2 in which the hexagonal basal plane of the CdI_2 lies parallel to the substrate, but with the unit cell rotated by $\simeq 7°$ with respect to the [110]. There are two domains, one either side of this direction, but there are no domains at $\pm 7°$ of the [1$\bar{1}$0] direction (see figure 11). The epitaxial layer evaporates at 403 K leaving a $p(2 \times 1)$ structure identical to that formed during adsorption. This structure then decomposes to a (1×1) $Cd_x I$ layer at 443 K ($x \geqslant 0.5$) in which the stoichiometry is probably CdI. The electron beams used for LEED and AES induced no detectable changes in any of the adsorbed surfaces formed by CdI_2. This implies that any electron stimulated desorption (ESD) process has a very low cross section, as our UPS studies both before and after LEED/AES would have detected any changes caused by the incident electron beams.

2. Experimental details

The experiments were carried out in two stainless-steel UHV chambers which have been described previously [6, 7]. Briefly, one chamber housed a four-grid retarding-field analyser (RFA) which was used for LEED and AES (using lock-in techniques and 3 V RMS modulation of the sample), while the other contained a three-grid RFA for LEED and a 50 mm mean radius concentric hemisphere analyser (CHA) for angle-resolved AES and UPS using pulse counting. For LEED the incident beam was $\simeq 1$ mm∅, while for Auger it was $\simeq 1.5$ mm∅ and 2 keV with both beams $\leqslant 10$ μA. The CHA was used in a fixed retard ratio mode of 10 for AES, and a fixed analyser transmission mode of 15 eV for UPS. The angles of incidence of the electrom beam and the He I beam were 45° to the surface normal and all spectra were taken along the surface normal unless stated otherwise.

Cadmium iodide was generated in vacuum by heating a cast pellet of AgI(95%)/CdI_2(5%) (wt%) at 443 K in a short (5 cm) tube. The same pellet and tube

were used for the all experiments reported here, the pellet-to-sample distances being 25 cm (UPS chamber) and 22 cm (LEED/AES chamber), with impingement along the surface normal. Assuming an inverse square law (which must hold for conservation of mass), the different sample-to-pellet distances should have caused a 23% difference in flux at the sample. Care was taken to use the same pellet temperature at all times so that, within experimental error, time (in either chamber) was directly proportional to exposure. The molecular flux was monitored with a quadrupole mass spectrometer and only fragments of CdI$_2$ were observed, no evaporated Ag was observed.

The sample used was a $\simeq 1$ cm^2, 500 μm thick wafer of InSb(001) (MCP Electronics UK Ltd) which had been mechanically polished and chemically etched prior to insertion in the vacuum chamber. It could be heated and cooled and was cleaned by Kr$^+$ bombardment at 573 K, to produce either the c(8 × 2) structure, or the streaky (4 × 2) structure, depending on which chamber was used. Note that the 8× periodicity lies in the [1$\bar{1}$0] direction (see figure 11(*a*)). For more details of the sample preparation and cleaning, see [8].

3. Results

3.1. Adsorption

CdI$_2$ was deposited onto the clean surface at 308 K by turning the sample to face the source for 30 minutes and then turning the sample away from the source for analysis. The source was held at the deposition temperature throughout the experiment as the vapour pressure of CdI$_2$ at room temperature, due to material adsorbing on the chamber walls and then desorbing, was too low to contribute to adsorption at the sample. The angle-integrated (measured with an RFA) In 404 eV, Sb 454 eV, Cd 376 eV and I 511 eV Auger peak-to-peak heights are shown as a function of exposure time in figure 1, along with the structures observed by LEED at the corresponding exposure. There is a rapid diminution of the In and Sb peaks with a concurrent rise in the Cd and I peaks. After 500 minutes the substrate In and Sb peaks were unobservable, while the Cd and I peaks had reached their saturation values. LEED showed that after 30 minutes the initial (4 × 1) structure had been replaced by a sharp, bright p(2 × 1). This structure reached its greatest perfection after 60 minutes, figure 3 (upper panel), with an In:Sb:Cd:I Auger peak-to-peak height ratio of 1:0.86:0.41:0.24 (last three all ±0.05). Further adsorption of CdI$_2$ produced a deterioration of the p(2 × 1) structure with the fractional order spots fading to leave a (1 × 1) structure with a high background and fairly dim integral order spots from the substrate. The (1 × 1) structure was still visible after 120 min, but further exposure then produced extra spots with hexagonal symmetry. After 250 min the substrate (1 × 1) structure was no longer visible, the hexagonal structure remaining on its own, figure 3 (middle panel). The hexagonal structure consisted of rather sharp bright spots on a moderately low background, distributed on two hexagonal nets which were offset by $\simeq 7°$ on either side of the [1$\bar{1}$0] direction of the substrate. In some experiments extra spots were seen oriented exactly along the [1$\bar{1}$0] direction, and exactly between the pairs of spots formed by the offset hexagonal nets, figure 3 (middle panel).

Further adsorption produced no further structures. If the adsorption is layer by layer, as would be expected for the growth of a layered compound, then the substrate intensities will be governed by an equation of the form $I = I_0 \exp(-d/\lambda)$ and the overlayer intensities by $I = I_0(1 - \exp(-d/\lambda))$ where d is the layer thickness, λ is
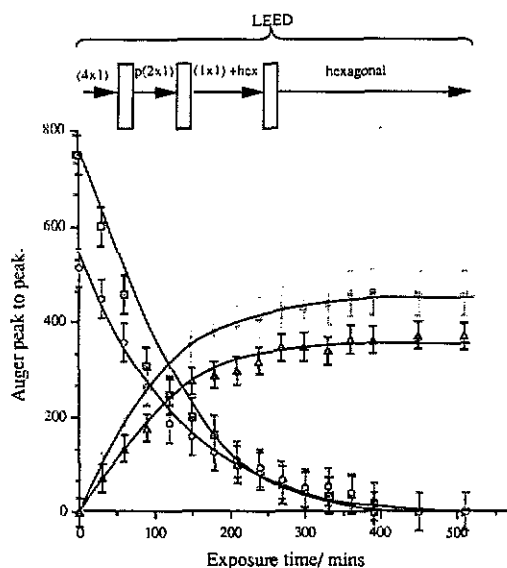
Figure 1. Angle-integrated Auger peak-to-peak heights versus CdI_2 exposure in minutes. Open squares represent In 404 eV, open circles Sb 454 eV, open triangles I 511 eV and filled diamonds Cd 376 eV. Also shown are the corresponding LEED structures.

the average effective mean free path over the solid angle studied for the particular Auger electron, I_0 the Auger intensity from the pure material (for the overlayer this is the saturated value I_{sat}) and I the intensity for thickness d. For a uniform deposition rate d is proportional to time so a plot of $\ln I$ (or $\log(I_{sat} - I)$) versus t should be a straight line with a gradient of $-k/\lambda$, where k is the growth rate in Å s^{-1}. Figure 2 shows that these plots are, indeed, linear. Each layer of bulk CdI_2 contains one molecule per 15.57 Å^2, while it is argued below that the $p(2 \times 1)$ contains one molecule per 20.98 Å^2. It took 60 min for the best $p(2 \times 1)$ to form, i.e. $60 \times 20.98/15.57 = 80.84$ min for one layer of CdI_2 to be deposited. The unit cell of CdI_2 has $c = 6.84$ Å, giving $k = 0.085$ Å min^{-1}. The mean free paths through CdI_2 are then calculated to be $\lambda_{In} = 9.4$ Å, $\lambda_{Sb} = 11.5$ Å, $\lambda_{Cd} = 6.9$ Å and $\lambda_I = 8.6$ Å. These agree rather well with the literature values of $\lambda_{In} = 10.8$ Å and $\lambda_{Sb} = 11.5$ Å [9] for Auger electrons passing through InSb.
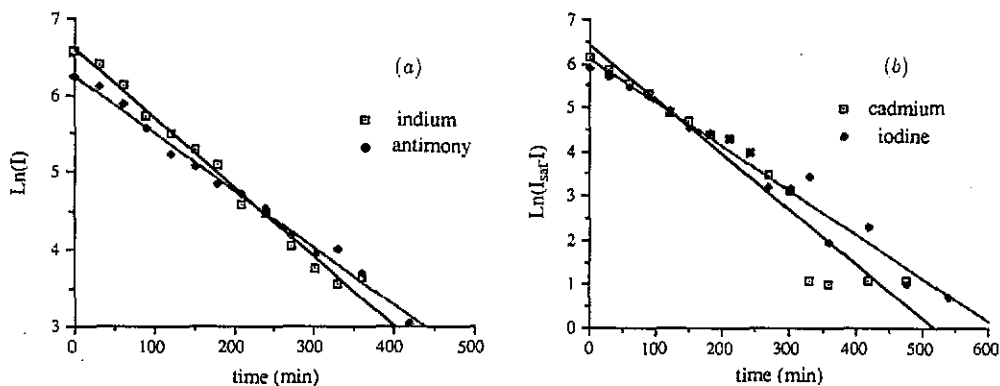

Figure 2. (a) Log I versus t plots for the In and Sb Auger peaks. (b) Log $(I_{sat} - I)$ versus t plots for the Cd and I Auger peaks in figure 1.
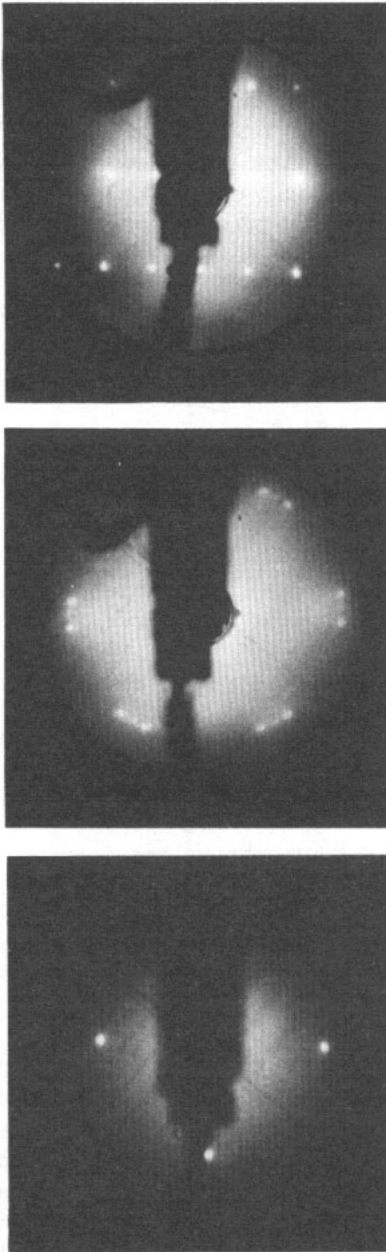
Figure 3. LEED patterns. Upper panel: InSb(001)–p(2 × 1) CdI$_2$ (50 eV). Middle panel: InSb(001)–hexagonal epitaxial CdI$_2$ (42 eV), two domains. Lower panel: InSb(001)–(1 × 1) CdI formed during desorption (50 eV).
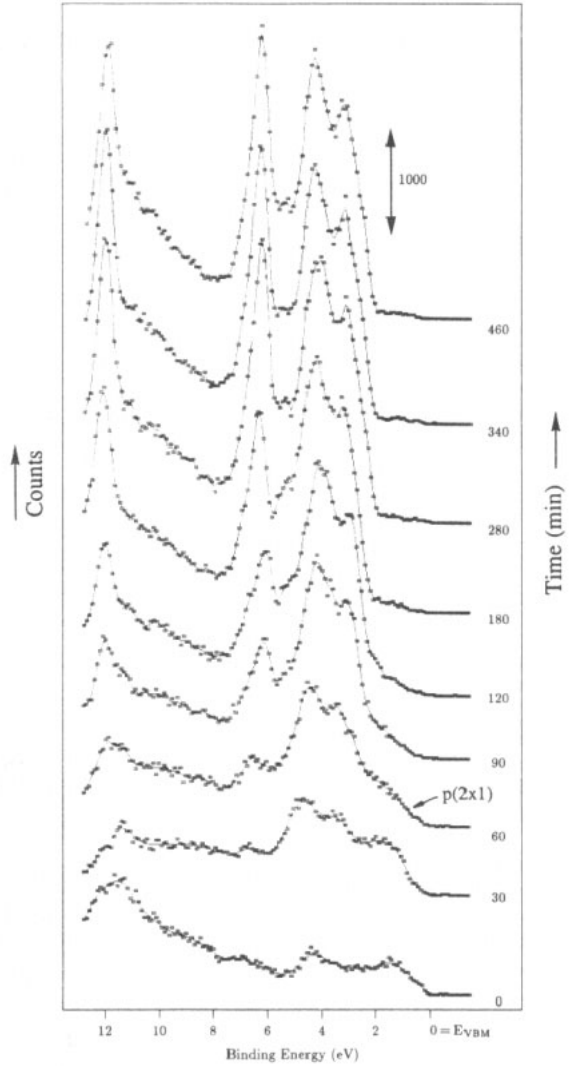
Figure 4. He I spectra for CdI$_2$ adsorption on InSb(001) c(8 × 2). Binding energies are measured relative to the valence band maximum of the clean surface. Spectra recorded at normal emission with photons incident at 45° in the (110) plane. The smoothed line is to guide the eye.

The adsorption was also monitored using angle-resolved photoelectron spec-

troscopy using unpolarised He I radiation. Figure 4 shows a nested plot of ARUP spectra for adsorption on the c(8 × 2) reconstruction. During initial adsorption there was rapid growth of two peaks at 3.3 and 4.2 eV (referenced to the valence band maximum (VBM) of the substrate). A third peak at 6.3 eV grew rather slowly at first, and then accelerated to eventually become larger than the first two peaks after 200 min exposure. A fourth peak at 11.8 eV initially grew even more slowly than the 6.3 eV peak, but its growth then also accelerated to become, eventually, larger than the two peaks at 3.3 and 4.2 eV. A small feature at 5.1 eV became visible after 180 min of CdI$_2$ exposure.
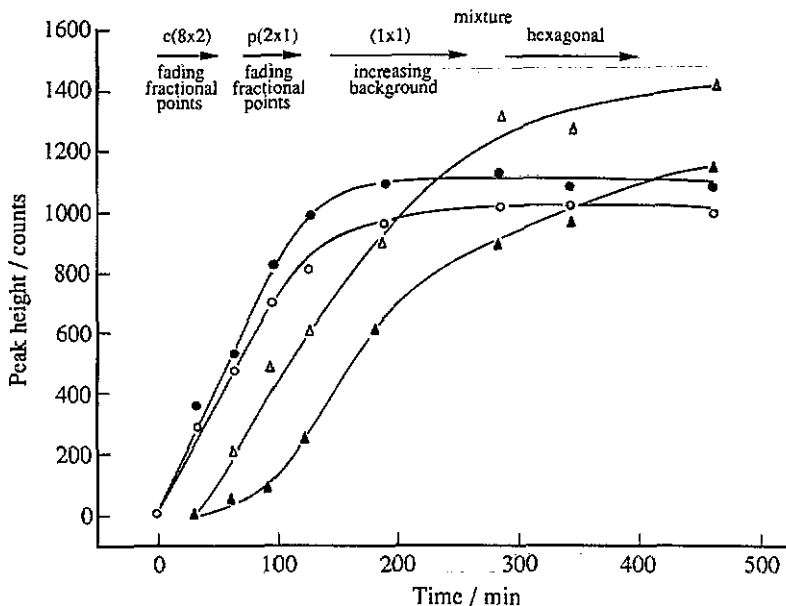

Figure 5. Growth of the 3.3 eV (open circles), 4.2 eV (filled circles), 6.3 eV (open triangles) and 11.8 eV (filled triangles) photoemission peaks from figure 4, above background.

Figure 5 shows the heights of these peaks above background (defined as the clean surface spectrum) as a function of exposure with the corresponding LEED patterns. The 3.3 and 4.2 eV peaks grew linearly during the formation and fading of the p(2×1) structure and became constant in intensity just as the p(2 × 1) structure disappeared. The 6.3 and 11.8 eV peaks, in contrast, continued to rise and only became saturated after $\simeq$ 500 min, the same exposure as that required to saturate the Cd and I Auger signals. There was a noticeable shift in just one of the peaks from 6.3 eV to 6.5 eV between 120 and 180 min, which occurred as the p(2 × 1) pattern was lost.

3.2. Desorption

Figure 6 shows the Auger peak-to-peak heights of I, Cd, Sb and In as a function of temperature as a multilayer surface ($\geqslant$ 500 min exposure) of CdI$_2$ on InSb(001), exhibiting the hexagonal structure, was heated to 533 K (the sample was heated to a given temperature and then allowed to cool prior to taking an Auger spectrum). Between 393 and 413 K there was a rapid decrease of the Cd and I Auger peak signals

to $\simeq 50\%$ of their initial values and the abrupt emergence of the Sb and In Auger peaks. The LEED pattern also changed from the hexagonal structure to the p(2 × 1) structure at this temperature. It follows that bulk desorption of the CdI$_2$ multilayer occurred at this temperature. The In:Sb:Cd:I Auger peak-to-peak height ratios of the p(2 × 1) formed by desorption were the same, to within experimental error, as those for the p(2 × 1) formed during adsorption.
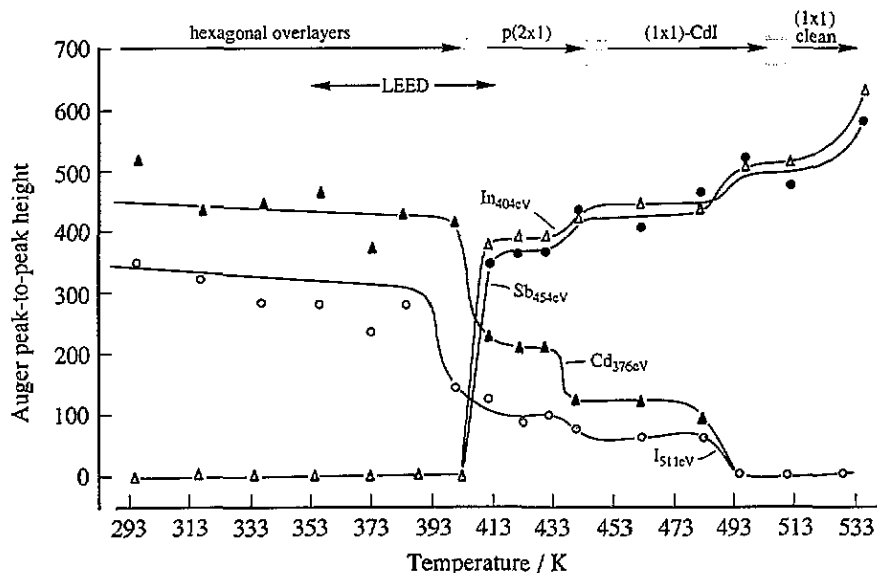

Figure 6. Peak-to-peak heights of the I 511 eV (open circles), Sb 454 eV (filled circles), In 404 eV (open triangles) and Cd 376 eV (filled triangles), Auger peaks versus temperature on heating a thick layer ($\geqslant$ 500 min exposure) in vacuum.

The p(2 × 1) structure remained stable over a short temperature range to 433 K, where the Cd and I peaks both decreased and the Sb and In peaks both increased abruptly. These small but distinct changes were accompanied by a change in LEED pattern to a sharp (1 × 1), figure 3 (lower panel). Finally between 473 and 498 K the Cd and I peaks fell below the detection level, and the Sb and In peaks underwent another rise. A (1 × 1) LEED pattern was observed for this clean surface. On reaching 523 K a mixed LEED pattern consisting of (1 × 3) and c(4 × 4) was observed as the Sb content of the surface increased. The behaviour from 498 K onwards was the same as that observed on desorbing pure iodine from InSb(001) [8]. The In:Sb Auger peak-to-peak height ratio of 1:0.92(±0.05) in figure 6 at 513 K is the same as that for the (1 × 1) surface formed by pure iodine desorption.

The same desorption sequence was studied using ARUPS, figure 7. Starting with the epitaxial, hexagonal multilayer of CdI$_2$ at 309 K, there was little change until 377 K is reached, apart from an increase in the intensity of the 11.8 eV peak. Between 377 and 401 K several changes occurred. The 11.8, 3.3 and 4.4 eV peaks all decreased, the 11.8 eV peak decreasing the fastest. At 401 K the p(2 × 1) structure was at its most perfect.

The 401 K spectrum in figure 7 is the same as the spectrum from the p(2 × 1) formed during adsorption in figure 4, confirming that the p(2 × 1) formed by adsorption or desorption are the same in all respects. Further heating brought about
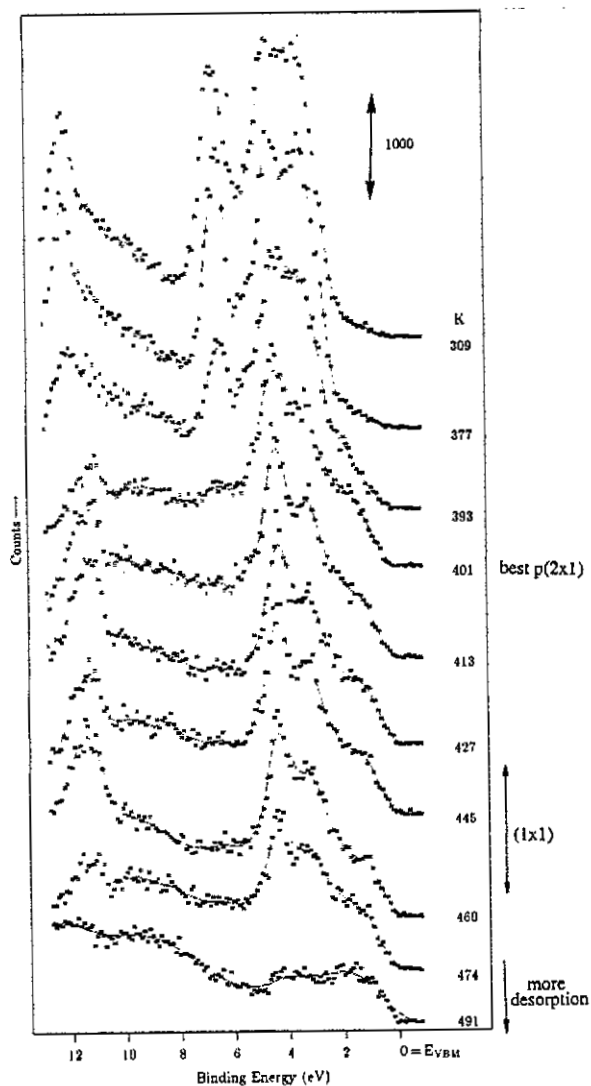
Figure 7. UP spectra taken during thermal desorption (heating then cooling to take the spectrum) of a thick, hexagonal, epitaxial layer of CdI_2 on InSb(001). The temperature is indicated on the right.

very little change in the cluster of peaks at 3–4 eV BE, but the peak at $\simeq 11.8$ eV for the 445 K (1×1) structure was markedly larger than the peak seen for the best $p(2 \times 1)$. Finally desorption recommenced and was complete by 493 K.

3.3. Angle-resolved photoemission spectra

He I angle-resolved photoemission spectra were recorded for the $p(2 \times 1)$, figure 9, and the hexagonal structure, figure 10. Spectra were recorded every 5° of emission angle (or less if substantial changes were occurring) with respect to the surface normal ([001]), in the (110) plane ($k_{\parallel}$ along $[1\bar{1}0]$) with the unpolarized radiation incident at 45° to the surface normal in the same plane, figure 11(a).

4. Discussion

Each layer of CdI$_2$ consists of a hexagonal net of cadmium atoms in the octahedral holes between two hexagonal nets of iodine atoms. Of the many possible polytypes which can be formed by different stacking sequences of these layers [10], we shall consider the simplest in which the unit cell is a hexagonal prism one I–Cd–I layer high [11]. The bonding within the I–Cd–I layer is strong and mainly ionic in character, while the bonding between the composite layers is of the weaker van der Waals type. Some crystallographic distances for solid CdI$_2$ are shown in table 1.

Table 1. Crystallographic parameters for CdI$_2$ in Å [11]. a and c refer to the unit cell, and should not be confused with meshes a, b and c used in the remainder of the text.

a	c	Cd–Cd	Cd–I	I–I, intralayer	I–I, interlayer
4.24	6.84	4.24	2.99	4.24	4.21

From the LEED pattern for the hexagonal epitaxial layer of CdI$_2$, figure 3 (lower panel) and figure 11(b), the ratio of the hexagonal unit mesh length (b^*) to the square substrate unit mesh length (a^*) in reciprocal space was found to be 1.3 ± 0.1. For a square and hexagonal net

$$b^*/a^* = 1.1547(a/b).$$

For $b = 4.24$ Å (CdI$_2$), table 1, and $a = 4.58$ Å (unreconstructed InSb(001) surface) $b^*/a^* = 1.247$, which is within the error limits of the experimental value. It follows that the CdI$_2$ grows with its hexagonal basal plane parallel to the InSb(001) surface. Figure 12 shows the real space diagram of this arrangement. By rotating the adlayer CdI$_2$ 7.46° with respect to the substrate, and contracting the lattice by 1.5%, the substrate and adsorbate lattice points align along the thick lines, the alignment repeating every two substrate unit meshes in the a_1 direction, [1$\bar{1}$0]. There is also exact coincidence every four substrate unit meshes in the same direction.

Orientational relationships (OR) between two bulk phases in precipitation systems have been observed for many years in which low-index planes lie parallel with particular directions within the planes aligned. For instance in the Nishiyama–Wassermann (NW) OR FCC(111)‖BCC(110) with FCC[0$\bar{1}$0]‖BCC [001], giving the structure two mirror planes, figure 8(a). If the two nets were rotated by 5.26°, figure 8(b), the new alignment would be a Kurdjumov–Sachs (KS) OR. The angle of 5.26° depends on the 60° and 54.74° angles in the FCC(111) and BCC(110) nets, and does not depend on the lattice constant. A full description of these ORs and others is given by Dahmen [12].

Bruce and Jaeger [13] describe a method of predicting whether a particular NW or KS OR will occur for a particular metal–metal system using the moiré fringes generated by superposition of the two nets. van der Merwe [14, 15] has carried out extensive calculations on the FCC(111)‖BCC(110) system and shown that three energy minima exist, two at the NW angle of 0° and the other at 5.26° for the KS. Ramirez *et al* [16] have also calculated the energy versus angle, position, separation and lattice constant ratio for the FCC(111)‖BCC(110) system using both a short-range exponentially decaying potential, and a Lennard-Jones potential. They also found
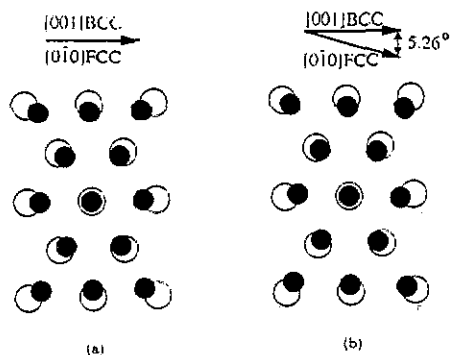
Figure 8. (*a*) Nishiyama–Wassermann orientational relationship. (*b*) Kurdjumov–Sachs OR.

three minima, two corresponded to an angle of 0° at two different lattice constant ratios, both being NW ORs, the third at an angle of 5° corresponded to the KS OR. Interestingly they found that the positioning of the two lattices had little effect on the energy, only the angle and the lattice constant ratio were important.

Another approach to rotational epitaxy is given by McTague and Novaco [17]. They calculated the energy versus rotational angle for hexagonal noble-gas adlayers on graphite. In these systems the lateral interactions are greater than the corrugation of the adatom–substrate interaction. They found that minimum energy occurred for a small angle (a few degrees) between the adlayer net and what would have been a perfect $(\sqrt{3} \times \sqrt{3})R30°$ structure, in agreement with experiment.

For the CdI_2 (basal plane)/InSb(001) system the arrangement is hexagonal/square, which is a relatively unusual combination [24]. In figure 12(*b*), if the angle between a_2 and b_2 were zero, then one row of lattice points through the origin would align along the a_2 direction, the remaining points would be parallel but unaligned, figure 12(*b*). This is similar to an NW OR, in that it has two mirror planes and a precise alignment of lattice points from both nets in one direction. In figure 3 (middle panel) faint spots can be seen lying half-way between the ±7° spots which correspond to this structure.

Figure 12(*c*) shows the angles to the horizontal made by the lines which must align to produce figure 12(*a*), they are 63.4349° and 70.8934° for the square and hexagonal nets respectively. Thus a rotation of 7.46° will bring these two directions into alignment. The interface formed by this rotation has not only exact alignment of lattice points through the origin, but very close alignment of rows of points every $2a_1$. If the b net lattice parameter is slightly reduced from 4.24 Å to 4.17 Å, then these extra rows (marked by heavy lines in figure 12(*a*)) align exactly. This contraction would also lead to coincidence of lattice points along a_1 every $4a_1$. We are unable to say from our LEED patterns whether such a contraction has occurred or not. This structure is similar to the KS OR, in that a small angular rotation has aligned a row of lattice points, but markedly different in that the rows that have aligned are not close packed, as they are in the KS OR. The structure appears to be a balance between the loss of stability by aligning non-close-packed instead of close-packed rows through the origin and the gain from aligning (or nearly aligning) rows every $2a_1$.

Cadmium iodide has been studied previously in the solid [1, 2] and gas phase [18–20]. In the gas phase the molecule is a linear triatomic, I–Cd–I, with a Cd–I bond length of 2.56 Å [21]. The σ_g molecular orbital (MO) is the deepest, being strongly Cd–I σ bonding and weakly I–I σ bonding. The π_g is highest in energy, as it has
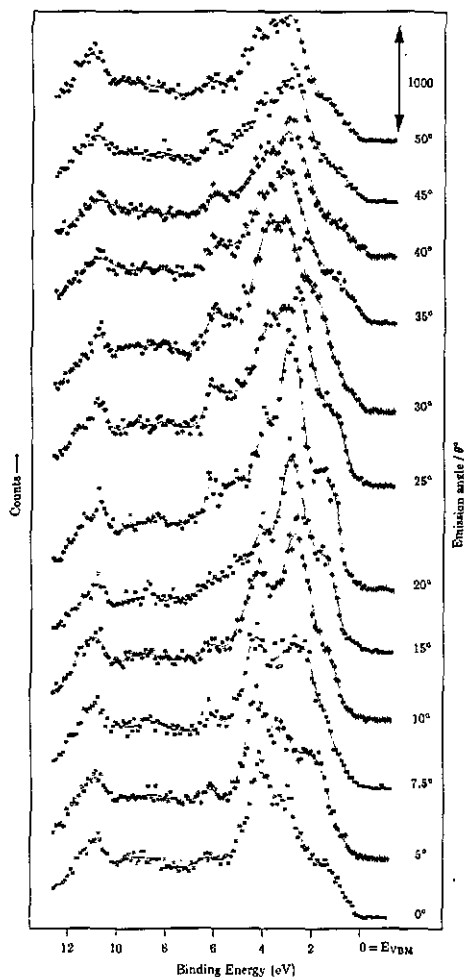
Figure 9. He I angle-resolved photoemission spectra of InSb(001)–p(2 × 1) CdI$_2$ with varying emission angle in the (110) plane. Photons incident at 45° to the normal in the same plane. The smooth line is to guide the eye.
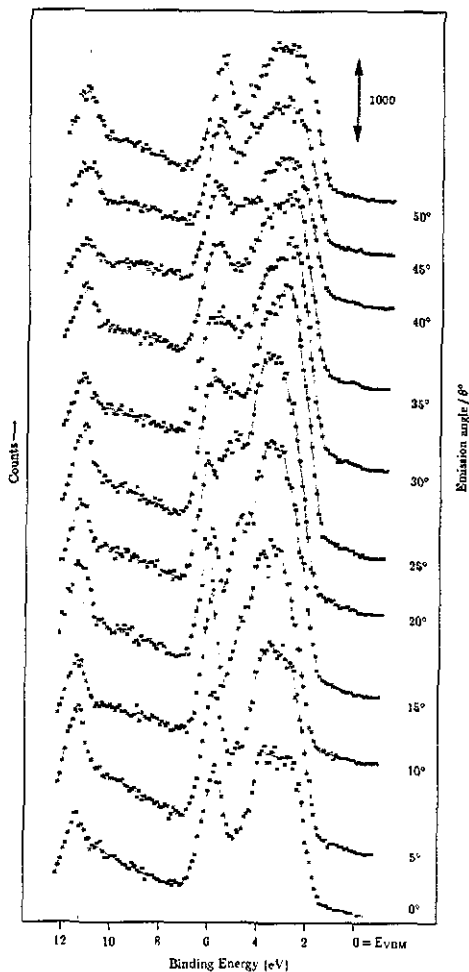
Figure 10. He I angle-resolved photoemission spectra of InSb(001)–hex-CdI$_2$ with varying emission angle in the (110) plane. Photons incident at 45° to the normal in the same plane.

zero contribution from the metal atomic orbitals and is also weakly I–I antibonding. Using similar arguments [20] the orbitals are expected to have the following order

$$[\text{Cd d}_{10}]\, \sigma_g^2 \qquad \sigma_u^2 \qquad \pi_u^4 \qquad \pi_g^4.$$

Spin–orbit splitting is expected, and observed for the Cd d and the π orbitals. The spectra of Boggess [18] and Berkowitz [19] are in close agreement, the latter also showing the spin–orbit-split Cd d orbitals using He II radiation. The $^2\Pi_{u,3/2}$, $^2\Pi_{g,1/2}$ and $^2\Pi_{u,1/2}$ are all within one broad band, making it difficult to identify individual peaks; however, Boggess has attempted to do this. The binding energies and peaks are shown in table 2.
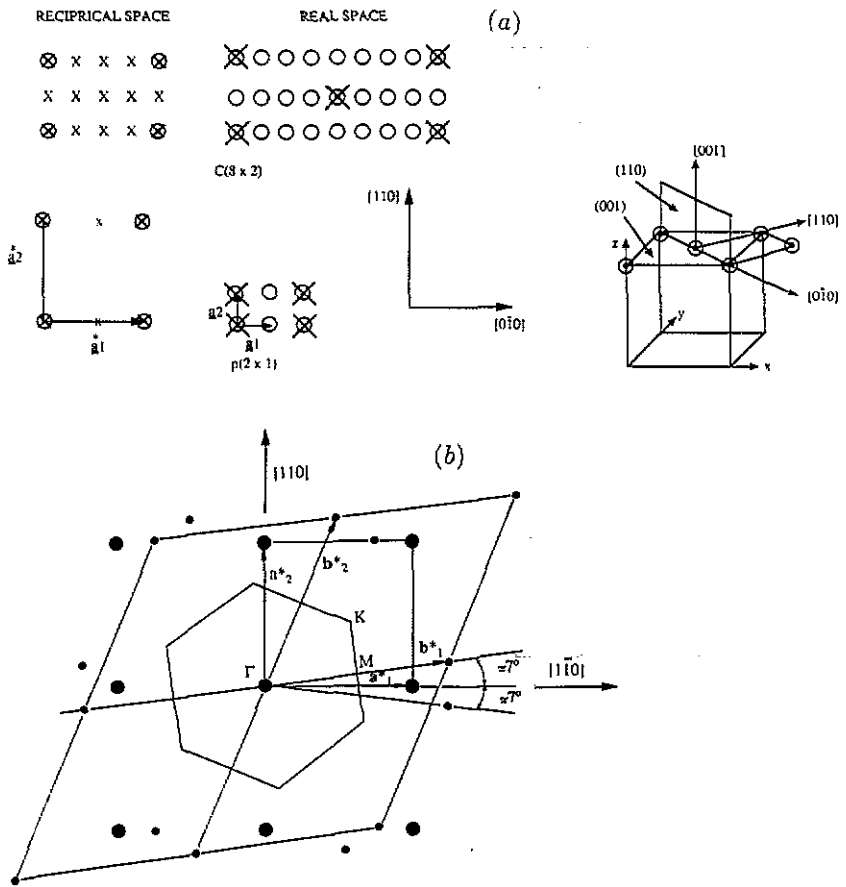
Figure 11. (*a*) Real- and reciprocal-space diagrams of the clean surface c(8 × 2) reconstruction and the p(2 × 1) CdI₂ structure showing how they are related to the bulk crystallographic directions, substrate net marked O, adlayer net X. Also shown is a sketch of the bulk InSb unit cell, illustrating the square unit mesh of the unreconstructed (001) surface and various planes and directions used in the text. (*b*) Reciprocal-space diagram of the hexagonal structure corresponding to the LEED pattern in figure 3(lower panel). One orientation of the adlayer (b^*) is shown in full (+7°), plus the reciprocal lattice points of the other orientation (−7°). Also shown is the first Brillouin zone of the hexagonal adlayer and the Γ, K and M points.

McCanny *et al* [1] have presented a theoretical and experimental study of the band structure of solid CdI₂. The band structure was calculated using a modified semi-empirical tight-binding method and the results compared to both angle-integrated and angle-resolved photoelectron data. As the forces between the composite I–Cd–I sandwich layers are weak, the band structure may be thought of as effectively two-dimensional, all dispersion occurring in $k_\parallel$; therefore the data from ARUPS, consisting of E_B versus $k_\parallel$, provide the complete band structure. However, this notion breaks down for orbitals oriented perpendicular to the layers, but involved in the strong bonding within the I–Cd–I layer. The He I ARUPS of pure CdI₂ measured by McCanny *et al* in the ΓM high-symmetry direction, figure 6 of [1], should be compared with figure 10 of this work which was taken along a line 7° off the ΓM direction, see
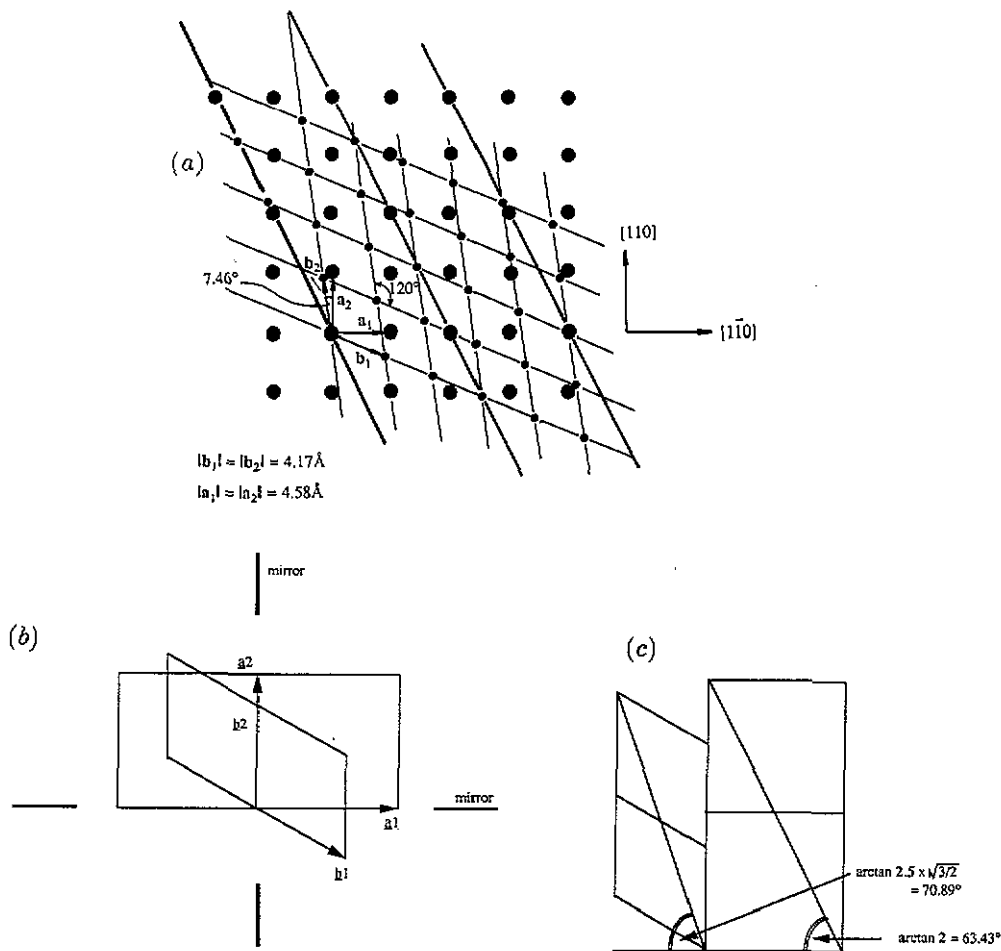
Figure 12. (*a*) Real-space diagram of the unreconstructed InSb(001) (a net) with the hexagonal epitaxial CdI_2 (b net) on top. The lattice points of the InSb(001) are shown by small circles, the lattice points of the CdI_2 by larger circles. Heavy lines show directions along which both sets of lattice points align. The figure has been drawn for an angle of 7.46° and $a = 4.58$ Å, $b = 4.17$ Å, which causes exact coincidence of the two meshes in the $[1\bar{1}0]$ direction every four substrate unit meshes. (*b*) Exact alignment of the vectors a_2 and b_2. (*c*) The angles of 63.4349° and 70.8934° described in the text.

figure 11. The spectra are, as might be expected, very similar. The rapidly dispersing peak at about 5 eV from 15° to 45° is particularly clear in this and McCanny's work. Table 2 shows the peak designations given by McCanny applied to the peak positions of the epitaxial hexagonal structure at the Γ point in this study. It can be seen from this table that the I_{p_z} (bonding) and I_{p_x} (antibonding) in the solid correspond to the σ_g and σ_u orbitals in the gas phase.

At this point we propose a model for the p(2 × 1) structure, and then discuss its consequences with respect to LEED structures, UPS and band structures. In a preliminary report [22] we suggested that the p(2 × 1) may be due to the adsorption of a highly distorted I–Cd–I sandwich, such that the hexagonal layer was distorted into a centred rectangle which matched the p(2 × 1) dimensions. This would require an

Table 2. Binding energies in eV. The columns are aligned so as to show the approximate equivalence of gas phase, chemisorbed and bulk states.

For gas-phase CdI₂ measured relative to vacuum

$^2\Pi_{g(3/2)}$	$^2\Pi_{u(3/2)}$	$^2\Pi_{g(1/2)}$	$^2\Pi_{u(2/2)}$	$^2\Sigma_u$	$^2\Sigma_g$	$^2D_{5/2}$	$^2D_{3/2}$	Reference
9.5	10.0	10.2	10.4	11.2	12.3			[18]
9.57	Broad——10.11——band			11.15	12.1			[20]
9.53		10.07		11.20	12.27	19.0	19.66	[19]
	Broad——10.21——band							[19]
——I_{px}——		——I_{py}——		I_{pz} (anti-bonding)	I_{pz} (bonding)	——Cd_d——		

InSb(001)–hex-CdI₂ for normal emission (this work)

	——2.8 to 4.4——			5.1	6.5		11.8	

InSb(001)–p(2 × 1)-CdI₂ for normal emission (this work)

| | 3.3 | | | 4.2 | ≈5.2 6.3 | | 11.8 | |

expansion of the hexagonal net from 15.57 to 20.98 Å², inducing considerable strain in the adlayer. Alternatively, one could consider how individual CdI₂ molecules might stack in a p(2 × 1). The molecule has a Cd–I bond length of 2.56 Å [21], to which should be added a van der Waals radius for iodine of ≃ 2.2 Å. If the molecule lay flat on the surface, it is only possible to fit one molecule per p(2 × 1) unit mesh (the molecule would lie diagonally in the unit mesh), giving a coverage of one iodine atom per substrate (1 × 1). However, the p(2 × 1) CdI₂ surface had an iodine Auger intensity 1.66 that of InSb(001)–(1 × 1) I formed by iodine adsorption [5], so this model cannot be correct. If the linear molecules are stood on end, vertical to the surface, it is easily possible to fit two molecules per unit mesh as shown in figure 13. Such a structure would have an iodine Auger peak intensity somewhat less than twice that of the (1 × 1) I structure, due to the attenuation of Auger electrons from the bottom layer by the upper layer, in agreement with experiment.
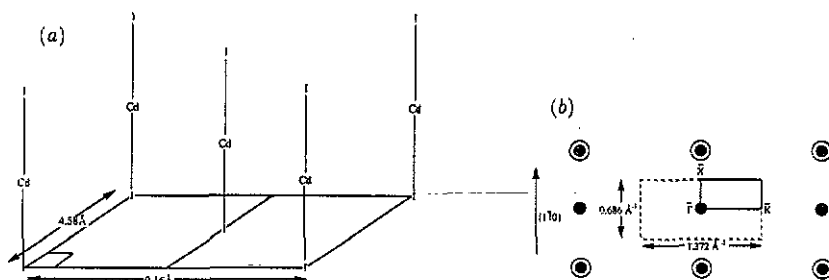

Figure 13. (a) Real-space diagram of the possible structure of the InSb(001)–p(2 × 1) CdI₂. (b) Reciprocal-space of the InSb(001)–p(2 × 1) CdI₂ showing surface Brillouin zone and high-symmetry points. Open circles are substrate (1 × 1) lattice points, filled circles p(2 × 1) lattice points.

The p(2 × 1) structure decomposed at elevated temperature, with a reduction in both iodine and cadmium Auger intensities, into a rather well formed (1 × 1) structure having the same iodine Auger intensity as the (1 × 1) I formed by pure iodine adsorption [5]. We can explain the reduction in the iodine Auger as being

due to the loss of the top layer of iodine in the p(2 × 1) structure, figure 13. If the cadmium atoms remained where they were, we would expect an increase in their Auger intensity because of the removal of the upper iodine layer. In fact the cadmium Auger intensity decreased, implying either desorption of some of the cadmium, or migration below the bottom layer of iodine atoms to the InSb interface. Figure 7 shows that the Cd d orbitals become intense, and rather broad for the (1 × 1) Cd$_x$I structure implying a significant change in bonding when compared with that in the hexagonal or p(2 × 1) structures, while the I_{p_z} (bonding) or σ_g of the CdI₂ becomes unobservable. The UPS of this (1 × 1) Cd$_x$I structure and the (1 × 1) structure formed by iodine on InSb(001) are shown in figure 14. The (1 × 1) I spectrum shows a strong I_{p_z} peak at 6.4 eV, while the (1 × 1) Cd$_x$I does not, and the $I_{p_{x,y}}$ regions of both spectra are similar in peak position, but not in intensity. For the (1 × 1) I structure we have assumed that the I_{p_z} is the main bonding orbital with the surface, as it undergoes a shift to 7.1 eV when a bulk surface iodide (mostly InI) is formed [8, 22]. Its absence in the (1 × 1) Cd$_x$I spectrum suggests markedly different bonding between the (1 × 1) iodine atoms and the surface. If as suggested above, there has been no loss of Cd on going from the p(2 × 1) to the (1 × 1) Cd$_x$I, then the surface stoichiometry would be CdI. This species, together with whatever substrate atoms are involved in the bonding, either has a very broad bonding orbital derived from the I_{p_z} or it is shifted into the $I_{p_{x,y}}$ region to lower binding energy (hence it is unobservable). Elucidation of the complete structure of the (1 × 1) Cd$_x$I must await further studies.

The ARUP spectra of the p(2 × 1), figure 9, are markedly different to those of the bulk compound and present a rather complex problem in peak identification due to structure from the InSb(001) substrate. In figure 15 clean surface spectra have been subtracted from the adlayer spectra for each angle. Several features can be seen. The large band at 3–4 eV ($I_{p_x} + I_{p_y}$) contains two features at about 3.3 and 4.2 eV which can be followed throughout the angular range, although at some angles (25° and 55°) three peaks are discernible. A shoulder at about 5 eV is due to the I_{p_z} (antibonding) or σ_u orbital, but is too indistinct to measure. The peak at 6.3 eV (I_{p_z} bonding or σ_g orbital) is slightly better resolved, but is still much weaker than in the bulk, making its behaviour difficult to perceive; however, it does not appear to disperse with angle.

The Cd d orbitals are also visible, though weak, and do not disperse. The two-dimensional band structure has been plotted using the 3.3 eV and 4.2 eV peaks, figure 16. The work function of the surface was found to be 0.23 eV less than that of the clean surface. Consequently a work function of 4.77 eV was used for calculating the electron kinetic energy and hence $k_\parallel$ [23]. The peak at 4.2 eV shows little dispersion, but that at 3.3 eV dispersed to smaller binding energy. Analysis was carried out along the $-\Gamma$–X direction, where the $-$X point lies at $k_\parallel = 0.343$ Å^{-1}. It can be seen that the dispersion is symmetrical about this point. If the $-\Gamma$–X direction is taken as the y direction, then the lack of dispersion of the p_x is readily understood, but the dispersion of the p_y to lower binding energy at $-$X is the opposite of what might be expected.

Irrespective of whether the linear CdI₂ were horizontal or vertical, with C_{2v} or C_{4v} symmetry (depending on orientation and site of adsorption), photoemission from all molecular orbitals is allowed with our geometry of unpolarized light at 45° to the surface and normal emission of photoelectrons.
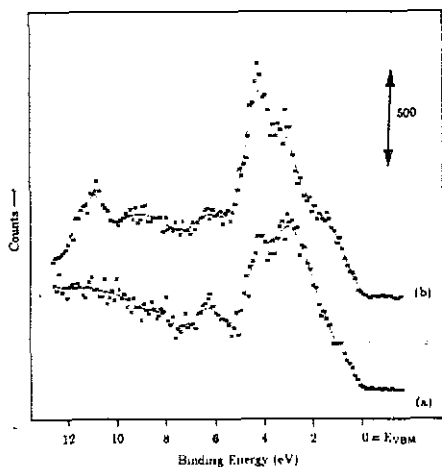
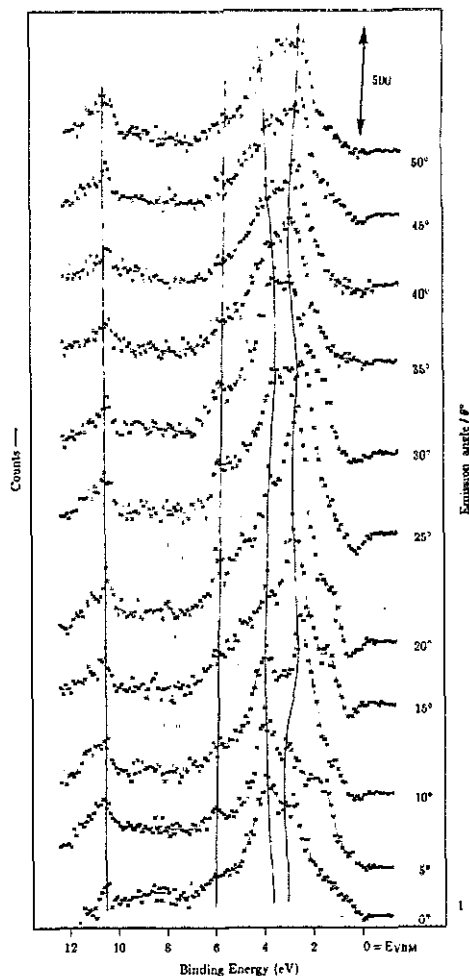**Figure 14.** He I UP spectra for (a) InSb(001)–(1 × 1) I and (b) InSb(001)–(1 × 1) CdI₂.

Figure 15. Angle-resolved He I UP spectra for the InSb(001)–p(2 × 1) CdI₂ after subtraction of the appropriate clean surface spectra at each angle. The smoothed line in each spectrum is to guide the eye.

5. Conclusion

Cadmium iodide adsorbs on InSb(001) to form a p(2 × 1) structure which probably consists of linear I–Cd–I molecules aligned nearly perpendicularly to the surface. Further adsorption leads to orientational relationship epitaxial growth of bulk CdI₂ with the basal plane of the CdI₂ parallel to the InSb(001) surface and an angle of $\simeq 7°$ between the hexagonal CdI₂ and square InSb(001) meshes. As far as we are aware this type of orientational relationship, which is similar to a Kurdjumov–Sachs OR but which does not align directions of close-packed atoms, has not been observed before. On desorbing the epitaxial layer, the chemisorbed p(2 × 1) is reformed, which then undergoes further desorption to form a primitive (1 × 1) which is thought
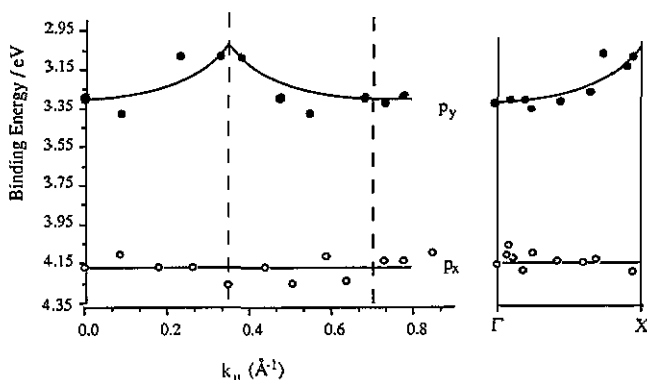
Figure 16. Band structure in the [1 -1 0] direction (Γ-X) for InSb(001)-p(2 × 1) CdI$_2$. BE is ±0.15 eV, $k_{\parallel}$ ± 0.05 Å^{-1}.

to consist of a (1 × 1) adlayer of iodine atoms with cadmium atoms below the iodine atoms and perhaps incorporated into the substrate. Further heating caused a complete loss of iodine and cadmium from this surface to produce an Sb-enriched clean surface. Further investigations involving the other cadmium halides and lead iodide are planned, to investigate this type of orientational relationship epitaxy.

Acknowledgments

References

[1] McCanny J V, Williams R H, Murray R B and Kemeny P C 1977 *J. Phys. C: Solid State Phys.* **10** 4255
[2] Bordas J, Robertson J and Jakobsson A 1978 *J. Phys. C: Solid State Phys.* **11** 2607
[3] Weast R C (ed) 1978 *CRC Handbook of Chemistry and Physics* 58th edn (Boca Raton, FL: Chemical Rubber Company)
[4] John P, Miller T and Chiang T-C 1989 *Phys. Rev.* B **39** 1730
[5] Mowbray A P and Jones R G 1990 *Vacuum* **41** 672
[6] Singh N K and Jones R G 1990 *Surf. Sci.* **232** 229
[7] Jones R G and Tong A W L 1987 *Surf. Sci.* **188** 87
[8] Mowbray A P, Jones R G and McConville C F 1991 *J. Chem. Soc. Faraday Trans.* **87** 3259
[9] Mackey K J 1988 *PhD Thesis* University of Wales, College of Cardiff
[10] Trigunayat G C and Chada G K 1971 *Phys. Status Solidi* a **4** 9
[11] McCanny J V, Williams R H, Murray R B and Kemeny P C 1977 *J. Phys. C: Solid State Phys.* **10** 4255
[12] Dahmen U 1982 *Acta Metall.* **30** 63
[13] Bruce L A and Jaeger H 1977 *Phil. Mag.* A **36** 1331; 1978 *Phil. Mag.* A **37** 337; 1978 *Phil. Mag.* A **38** 223
[14] van der Merwe J H and Braun M W H 1985 *Appl. Surf. Sci.* **22–3** 545
[15] Bauer E and van der Merwe J H 1986 *Phys. Rev.* B **33** 3657
[16] Ramirez R 1984 *Phys. Rev.* B **30** 6208
[17] McTague J P and Novaco A D 1979 *Phys. Rev.* B **19** 5299
[18] Boggess G W, Allen J D Jr and Schweitzer G K 1973 *J. Electron Spectrosc. and Relat. Phenom.* **2** 467

[19] Berkowitz J 1974 *J. Chem. Phys.* **61** 407
[20] Cocksey B G, Eland J H D and Danby C J 1973 *J. Chem. Soc. Faraday Trans.* II **69** 1558
[21] Ball M C and Norbury A H 1974 *Physical Data for Inorganic Chemists* (New York: Longman)
[22] Mowbray A P and Jones R G 1991 *Appl. Surf. Sci.* **48–9** 27
[23] Williams R H, Srivastava G P and McGovern I T 1984 *Electronic Properties of Surfaces* ed M Prutton
      (Bristol: Adam Hilger) p 71
[24] Epitaxy data of inorganic and organic crystals *Landolt–Börnstein New Series* 1972 Group III, vol 8
      ed K-H Hellwege (Berlin: Springer)